

Substituent Effects on the Reaction of β -Benzoylalanines with *Pseudomonas fluorescens* Kynureninase

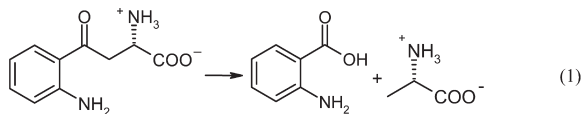
Sunil Kumar,^{†,§} Vijay B. Gawandi,^{†,||} Nicholas Capito,[‡] and Robert S. Phillips^{*,†,§}

[†]Department of Chemistry and [§]Department of Biochemistry and Molecular Biology, University of Georgia, Athens, Georgia 30602. ^{||}Present address: The Department of Biochemistry and Biophysics, Texas A&M University, College Station, TX 77843-2128.

Received June 14, 2010; Revised Manuscript Received August 5, 2010

ABSTRACT: Kynureninase is a pyridoxal 5'-phosphate-dependent enzyme that catalyzes the hydrolytic cleavage of L-kynurenine to give L-alanine and anthranilic acid. β -Benzoyl-L-alanine, the analogue of L-kynurenine lacking the aromatic amino group, was shown to be a good substrate for kynureninase from *Pseudomonas fluorescens*, and the rate-determining step changes from release of the second product, L-Ala, to formation of the first product, benzoate [Gawandi, V. B., et al. (2004) *Biochemistry* 43, 3230–3237]. In this work, a series of aryl-substituted β -benzoyl-DL-alanines was synthesized and evaluated for substrate activity with kynureninase from *P. fluorescens*. Hammett analysis of k_{cat} and $k_{\text{cat}}/K_{\text{m}}$ for 4-substituted β -benzoyl-DL-alanines with electron-withdrawing and electron-donating substituents is nonlinear, with a concave downward curvature. This suggests that there is a change in rate-determining step for benzoate formation with different substituents, from *gem*-diol formation for electron-donating substituents to C_{β} – C_{γ} bond cleavage for electron-withdrawing substituents. Rapid-scanning stopped-flow kinetic experiments demonstrated that substituents have relatively minor effects on formation of the quinonoid and 348 nm intermediates but have a much greater effect on the formation of the aldol product from reaction of benzaldehyde with the 348 nm intermediate. Since there is a kinetic isotope effect on its formation from β , β -dideuterio- β -(4-trifluoromethylbenzoyl)-DL-alanine, the 348 nm intermediate is proposed to be a vinylogous amide derived from abortive β -deprotonation of the ketimine intermediate. These results provide additional evidence for a *gem*-diol intermediate in the catalytic mechanism of kynureninase.

Kynureninase (kynase)¹ (EC 3.7.1.3) is a pyridoxal 5'-phosphate- (PLP-) dependent enzyme that catalyzes the hydrolytic cleavage of L-kynurenine to anthranilic acid and L-alanine (1) (eq 1). The reaction is a key step in the catabolism of L-tryptophan by *Pseudomonas fluorescens* and some other bacteria (2). The inducible kynase from *P. fluorescens*, a dimer with a subunit molecular weight of about 45000, has been cloned and expressed in *Escherichia coli* (3). In animals and some fungi, a similar constitutive enzyme reacts preferentially with 3-hydroxy-L-kynurenine in the catabolism of L-tryptophan (1). In eukaryotes, the kynurenine pathway is responsible for the de novo biosynthesis of NAD^+ , via the intermediacy of quinolinate. However, quinolinate is also a neurotoxin, due to its agonist effects on the *N*-methyl-D-aspartate receptor, and excessive levels of quinolinate have been implicated in the etiology of a wide range of diseases such as epilepsy, stroke, and neurological disorders, including AIDS-related dementia (4, 5). Thus, selective inhibitors of human kynase are of interest as possible drugs for the treatment of a range of neurological disorders (6).



It has been shown previously that β -benzoyl-L-alanine, which lacks the aromatic amino group of the natural substrate, is a

substrate for bacterial kynase (7), with k_{cat} and $k_{\text{cat}}/K_{\text{m}}$ values of 0.7 s^{-1} and $8.0 \times 10^4 \text{ M}^{-1} \text{ s}^{-1}$, respectively, compared to $k_{\text{cat}} = 16.0 \text{ s}^{-1}$ and $k_{\text{cat}}/K_{\text{m}} = 6.0 \times 10^5 \text{ M}^{-1} \text{ s}^{-1}$ for L-kynurenine. The rate-determining step in the reaction of β -benzoyl-L-alanine with kynase is C_{β} – C_{γ} bond cleavage to form the first product, benzoate, whereas the rate-determining step in the reaction of the natural substrate, L-kynurenine, is the release of the second product, L-alanine (8). Furthermore, β -benzoyl-L-alanine reacts with kynureninase to form a transient 348 nm intermediate in stopped-flow kinetic experiments. Addition of benzaldehyde together with β -benzoyl-L-alanine results in decay of the 348 nm complex and formation of a new quinonoid complex that absorbs at 494 nm (7). In the current work, we have synthesized a series of β -benzoyl-DL-alanines substituted with electron-withdrawing and electron-donating groups as probes of the reaction mechanism. These compounds were examined by steady-state and stopped-flow kinetics with *P. fluorescens* kynase. The results suggest that there is a change in the rate-determining step for benzoate formation from carbonyl hydration to C_{β} – C_{γ} bond cleavage with electron-donating and electron-withdrawing substituents, respectively.

EXPERIMENTAL PROCEDURES

Enzyme Purification. Kynase was purified as previously described from *E. coli* DH-5 α cells that were transformed with the pTZKYN plasmid containing the *kyn* gene cloned from *P. fluorescens* (3).

Steady-State Kinetics. The steady-state kinetic measurements were performed on a Cary 1E UV/vis spectrophotometer equipped with a 6 \times 6 Peltier thermoelectric cell changer, controlled by a PC using software provided by Varian instruments. Substrate

*To whom correspondence should be addressed at the Department of Chemistry, University of Georgia. E-mail: rsphillips@chem.uga.edu. Phone: (706) 542-1996. Fax: (706) 542-9454.

¹Abbreviations: kynase, kynureninase (EC 3.7.1.3); PLP, pyridoxal 5'-phosphate; PMP, pyridoxamine 5'-phosphate.

Table 1: Spectroscopic Data for Substituted β -Benzoylalanines

substituent, X	molar extinction coeff ($M^{-1} cm^{-1}$)	λ_{max} (nm)
(1) 4-OMe	2600	280
(2) 4-Me	1660	259
(3) 4-Cl	2600	247
(4) 4-CF ₃	4442	243
(5) 2-Cl	2600	247
(6) 2-F	1946	243
(7) 2-OMe	1504	255

activities of all the new compounds were measured at their respective absorption maxima (Table 1). All the assays were performed at 37 °C in 0.04 M potassium phosphate, pH 7.8, containing 40 μ M PLP, in a total volume of 700 μ L. K_m , k_{cat} , and k_{cat}/K_m values were calculated using the FORTAN program, HYPER, of Cleland (9).

Stopped-Flow Kinetics. Rapid-scanning stopped-flow kinetic experiments were performed on an OLIS RSM-1000 instrument at ambient temperature. This instrument is capable of collecting rapid-scanning data at 1000 scans per second over the wavelength range from 200 to 800 nm, with a dead time ≤ 2 ms. The enzyme solutions contained 1 mg/mL *P. fluorescens* kynase in 0.04 M potassium phosphate, pH 8.0. These were mixed with solutions of 1 mM compounds 1–7 in the same buffer. When benzaldehyde was present, it was added to the substrates at 10 mM. The wavelength region from 300 to 560 nm was used to analyze the data by global fitting using the Global Works program (10) provided by OLIS, Inc.

Synthesis of Substrate Analogues. β -(4-Methylbenzoyl)-DL-alanine (**1**). 2-Bromo-1-(4-methylphenyl)ethanone (**1b**). CuBr₂ (3.19 g, 14.2 mmol) (*11*) was heated at reflux in 10 mL of EtOAc with stirring. To this was added 4-methylacetophenone (**1a**, 2.36 g, 11.4 mmol) in 10 mL of CHCl₃. The reaction mixture was heated at reflux for 5 h and then cooled to room temperature. CuBr and CuBr₂ residues were filtered, and the filtrate was decolorized with activated charcoal, filtered again through a bed of Celite, and washed with EtOAc (4 \times 50 mL). The solvent was removed under reduced pressure to give yellow crystals. Further purification by recrystallization gave 1.4 g (58%) of the brominated product **1b**, mp 52–56 °C. ¹H NMR (CDCl₃) δ (ppm) 2.335 (s, 3H), 4.28 (s, 2H), 7.161 (d, 2H), 7.915 (d, 2H).

Ethyl 4-(4'-Methylphenyl)-4-oxo-2-acetamido-2-ethoxycarbonylbutyrate (**1c**). Sodium hydride (1.39 g, 34.9 mmol, 2.5 equiv) (60% in mineral oil) was suspended in dry DMF (14 mL). A solution of diethyl acetamidomalonate (4.56 g, 21 mmol, 1.5 equiv) in dry DMF was added. The solution was stirred at 0 °C under a nitrogen atmosphere for 3 h until the anion had formed. A solution of 2-bromo-1-(4-methylphenyl)ethanone (**1b**, 13.9 mmol, 2.78 g) in dry DMF (10 mL) was then added, and the solution was warmed to room temperature and stirred overnight under nitrogen. The reaction mixture was poured into distilled water (100 mL), acidified in an ice bath to pH 3 with 1 M hydrochloric acid, and extracted into diethyl ether (4 \times 70 mL). The ether extracts were dried over MgSO₄, and the solvent was removed under reduced pressure to give white crystals of ethyl 4-(4'-methylphenyl)-4-oxo-2-acetamido-2-ethoxycarbonylbutanoate (**1c**). Yield 2.3 g (45%). ¹H NMR (CDCl₃) δ (ppm) 1.27–1.29 (t, 6H), 1.84 (s, 3H), 2.34 (s, 3H), 3.51 (s, 2H), 4.13 (m, 4H), 7.18 (d, 2H), 7.38 (d, 2H), 7.92 (s, 1H).

β -(4-Methylbenzoyl)-DL-alanine (**1**). Ethyl 4-(4'-methylphenyl)-4-oxo-2-acetamido-2-ethoxycarbonylbutanoate (**1c**, 1.6 g,

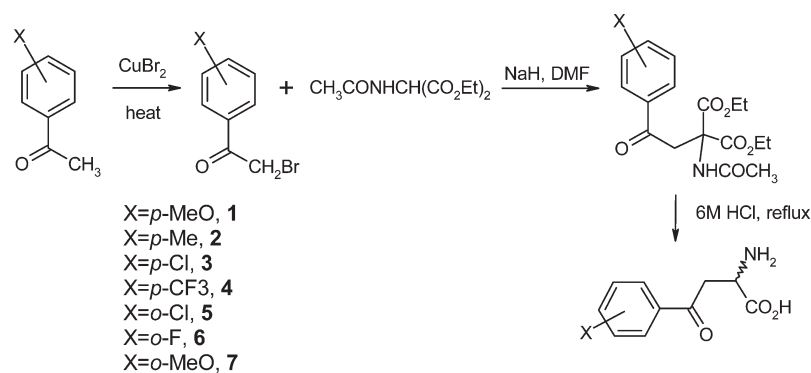
4.7 mmol) was dissolved in 1,4-dioxane (50 mL), and 6 M hydrochloric acid (70 mL) was added. The reaction was heated under reflux for 8 h until no starting material was visible by TLC (silica gel, petroleum ether/EtOAc, 1:1). The solution was then cooled and washed with EtOAc (50 mL). The aqueous phase was concentrated under reduced pressure to give a brown syrup, which was triturated with acetone to produce β -(4-methylbenzoyl)-DL-alanine hydrochloride as an off-white crystalline solid. The hydrochloride product was then applied to a Dowex-50 cation-exchange column and eluted with 1 M NH₃ to yield the amino acid (**1**). Yield 0.60 g (65%). ¹H NMR (D₂O + DCl) δ (ppm) 2.34 (s, 3H), 3.73–3.74 (dd, 2H), 4.34–4.36 (t, 1H), 7.82 (d, 2H), 7.16 (d, 2H).

Deuteration of 4-Trifluoromethylbenzoylalanine. β -(4-Trifluoromethylbenzoyl)alanine (0.0204 g) was dissolved in 5 mL of D₂O containing 10 μ L of 14.2 M NaOD. A sample was removed and examined by ¹H NMR after 4 h, and the β -hydrogen resonances were not detected. Glacial acetic acid (10 μ L) was then added to adjust the pH to 6, and the solution was left at 4 °C for the deuterated product to crystallize. After standing over the weekend, the fine suspension of crystals was filtered, washed with a little cold water, and air-dried to give 0.0073 g. ESI MS: 264 ($M + 1$), as predicted for the dideuterio compound.

RESULTS

Chemistry. All of the substituted β -benzoyl-DL-alanines were synthesized based on our previously published procedure (7) (Scheme 1) used to prepared the parent compound. Compounds 1–7 were obtained starting from the α -bromination of the corresponding commercially available substituted acetophenones (**1a–7a**) with CuBr₂ (*11*). In contrast to the literature (*11*), which states that the α -monobrominated product is exclusively obtained, we generally obtained a mixture of α -monobrominated (**1b–7b**) and α,α -dibrominated acetophenones. However, the α -monobrominated acetophenone was readily separated from the undesired dibrominated product either by recrystallization or silica gel column chromatography. Alkylation of the monobrominated acetophenone with diethylacetamidomalonate using sodium hydride as a base afforded the diethyl benzoylmethylacetamidomalonate (**1c–7c**). Attempts to alkylate diethylacetamidomalonate with bromoacetophenones using the more common reagent, sodium ethoxide in ethanol, gave poor yields. In some cases, a mixture of mono- and diethyl ester products were obtained after alkylation, along with other unknown byproducts, indicating that a partial Krapcho decarboxylation had occurred. The combined mono- and diester products were subjected to acid hydrolysis and decarboxylation to furnish the substituted β -benzoyl-DL-alanine hydrochloride, which was then neutralized or treated with Dowex-50 cation exchange resin to give the free racemic amino acids (**1–7**). The UV absorption properties of 1–7 used for the activity assays are summarized in Table 1. Details for the synthesis of compounds 2–7 are provided in the Supporting Information.

Steady-State Kinetics. All of the compounds tested (**1–7**) were found to be substrates for hydrolytic cleavage by *P. fluorescens* kynase, with varying degrees of efficiency (Table 2). We have shown previously that the K_m for β -benzoyl-L-alanine is half that of β -benzoyl-DL-alanine, indicating that the D-isomer does not interact significantly with kynureninase (7). The Hammett plot of $\log(k_{cat})$ and $\log(k_{cat}/K_m)$ against the substituent constants for the para-substituted compounds (**1–4**) shows a concave downward nonlinear relationship, which suggests that there is a change in the rate-determining step for compounds with strongly electron-donating or electron-withdrawing substituents (Figure 1).

Scheme 1: Synthesis of Substituted β -BenzoylalaninesTable 2: Steady-State Kinetic Parameters for Substituted β -Benzoylalanines

substituent, X	k_{cat} (s^{-1})	$k_{\text{cat}}/K_m \times 10^{-3}$ ($\text{M}^{-1} \text{s}^{-1}$)
(1) 4-OMe	0.38 ± 0.06	1.6 ± 0.28
(2) 4-Me	0.91 ± 0.06	28 ± 0.02
(3) 4-Cl	1.83 ± 0.78	18 ± 0.04
(4) 4-CF ₃	0.001 ± 0.0004	0.019 ± 0.003
(5) 2-Cl	0.08 ± 0.006	12 ± 2.8
(6) 2-F	0.06 ± 0.006	1.7 ± 0.2
(7) 2-OMe	0.05 ± 0.006	1.4 ± 0.25
H	0.7	80

Similar slopes are seen for both k_{cat} and k_{cat}/K_m in the electron-donating region, with $\sigma < 0$ ($\rho = 0.590 \pm 0.275$ and 0.455 ± 0.068 , respectively), while k_{cat} is more sensitive ($\rho = -4.238 \pm 1.12$) than k_{cat}/K_m ($\rho = -0.986 \pm 0.031$) to the effect of electron-withdrawing groups with $\sigma > 0$. The very low activity of the CF₃ derivative (**4**) was confirmed by ¹⁹F NMR of reaction mixtures, which showed a new resonance at -63.042 ppm, downfield of the resonance of **4** at -63.595 ppm, after overnight incubation. It is interesting that all of the 2-substituted β -benzoylalanines, 2-F, 2-Cl, and 2-MeO, are poor substrates (Table 2), even though the physiological substrate, kynurenine, has a 2-amino substituent.

Pre-Steady-State Kinetics. When β -benzoylalanine is mixed with *P. fluorescens* kynase in the stopped-flow spectrophotometer, the enzyme spectrum changes, and a new intermediate forms with a strong absorption peak at about 348 nm (7). Figure 2 shows the results of the reaction of β -(4-chlorobenzoyl)alanine (**3**) with *P. fluorescens* kynase in the stopped-flow spectrophotometer. The data in Figure 2A,B show a reaction very similar to that observed previously with β -benzoylalanine, with a 348 nm intermediate forming, concomitant with decay of the external aldimine at 420 nm (Figure 2A,B), and an isosbestic point at 388 nm. Similar results are seen with the trifluoromethyl analogue, **4** (Figure 3). The reaction of β, β -D₂-**4** exhibits a kinetic isotope of 1.88 ± 0.14 on the formation of the 348 nm intermediate (Figure 4B). There is also a significant equilibrium isotope effect on the formation of the 348 nm intermediate, since the steady-state absorption of the 348 nm intermediate is reduced (Figure 4A). Compounds **1–7** all form the 348 nm intermediate, at rate constants ranging from 2 to 20 s^{-1} ($1/\tau_1$, Table 3, and Figure 5), similar to the value of 9 s^{-1} seen previously with β -benzoylalanine (7).

The 348 nm intermediate formed with β -benzoylalanine was found previously to decay in the presence of benzaldehyde, and concomitantly a new quinonoid species with λ_{max} of 494 nm formed (7), derived from the aldol product, γ -phenylhomoserine. In the case of compounds **1–7**, the rate constant for reaction of

the 348 nm intermediate with benzaldehyde to form a quinonoid complex shows a much greater range of values than for its formation (Table 3). 4-Me- and 4-Cl-benzoylalanine (**2** and **3**) show reactivity similar to that of β -benzoylalanine ($1/\tau_2$, Table 3 and Figure 2D), while 4-MeO- and 4-CF₃-benzoylalanine (**1** and **4**) show much lower reactivity ($1/\tau_2$, Table 3 and Figure 3D). 2-Cl- and 2-F-benzoylalanine (**5** and **6**) react much more slowly ($1/\tau_2$, Table 3 and Figure 5D), and 2-MeO-benzoylalanine (**7**) did not show any detectable formation of the quinonoid species in the presence of benzaldehyde for at least 30 s. Thus, the reactivity of the 348 nm intermediates with benzaldehyde to form the 494 nm quinonoid intermediate in the stopped-flow experiments roughly parallels the k_{cat} activity for the substituted benzoylalanines in Table 2.

DISCUSSION

Kynase is one of a small group of enzymes that catalyze retro-Claisen-type reactions. This reaction is proposed to proceed via a tetrahedral intermediate on the γ -carbonyl carbon (1, 7, 8, 12–16). We showed previously that dihydrokynurenines (12, 13, 15) and *S*-phenylcysteine sulfones (14, 15) are potent competitive inhibitors of *P. fluorescens* kynase, with K_i values in the low micromolar to nanomolar range. These results suggested that a *gem*-diolate intermediate is involved in the reaction mechanism and that these inhibitors are transition-state analogues. Later, we found that β -benzoyl-L-alanine is a good substrate for kynase, but the rate-determining step is formation of the first product, benzoate (7), while the rate-limiting step in the reaction of L-kynurenine is release of L-Ala (8). In the present work, we prepared and examined a number of ring-substituted β -benzoyl-DL-alanines to probe the electronic effects on benzoate formation. Hammett analysis of the steady-state kinetic data for the para-substituted compounds (Figure 1) shows strongly downward curvature, indicating that there is a change in rate-determining step for benzoate formation with substituent.

The proposed mechanism of kynase involves formation of an external aldimine with PLP, followed by deprotonation of the α -C and reprotonation at C-4' to form a ketimine (Scheme 2). Addition of water to the γ -carbonyl of the ketimine forms a *gem*-diolate intermediate, followed by a retro-Claisen cleavage of the C $_{\beta}$ –C $_{\gamma}$ bond (Scheme 2). The stereochemistry of the retro-aldol reaction catalyzed by kynureninase with dihydro-L-kynurenine is consistent with an (*S*)-*gem*-diolate intermediate (13). According to the Dunathan hypothesis (17), the C $_{\beta}$ –C $_{\gamma}$ bond of the *gem*-diolate should be perpendicular to the π -system of the PMP-ketimine for cleavage of the C $_{\beta}$ –C $_{\gamma}$ bond to occur. Since there is only one catalytic base from the pH dependence of k_{cat}/K_m (8),

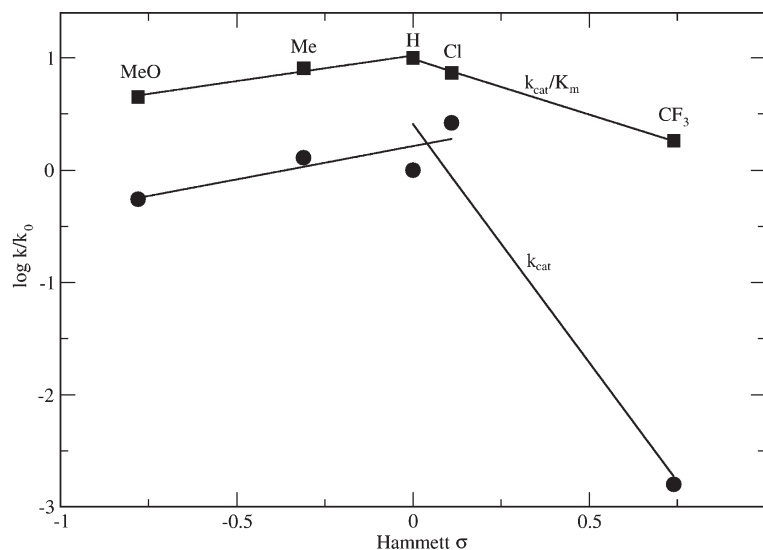


FIGURE 1: Hammett plot for reaction of substituted β -benzoylalanines. Key: circles, k_{cat} ; squares, k_{cat}/K_m . The lines were obtained by regression analysis, with the slopes indicated in the text.

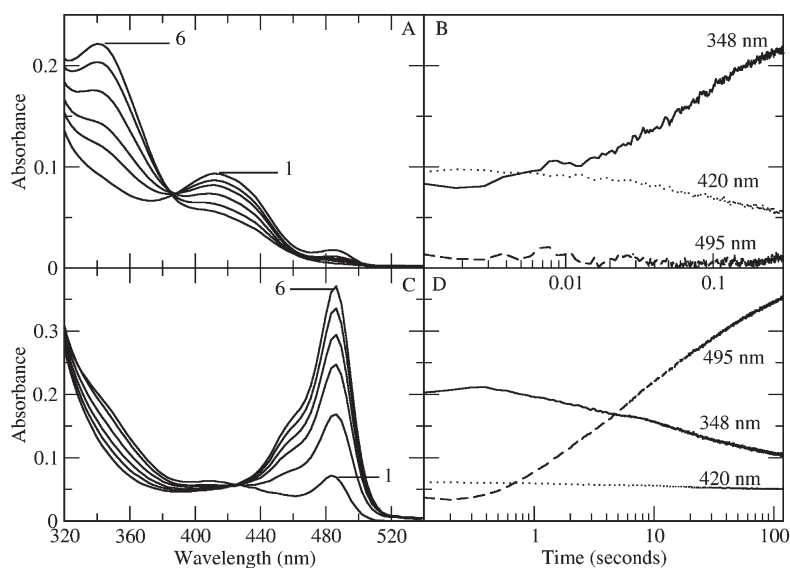


FIGURE 2: Reaction of β -(4-chlorobenzoyl)-DL-alanine (**3**) with *P. fluorescens* kynase in the stopped-flow spectrophotometer. Reactions contained 1 mg/mL kynase in 40 mM potassium phosphate, pH 8.0, 0.5 mM **3** (A, B, C, and D), and 5 mM benzaldehyde (C and D). (A) Reaction with 0.5 mM **3**. Curves are shown at 0.0008 s (1), 0.0308 s (2), 0.0808 s (3), 0.1608 s (4), 0.3208 s (5), and 0.6408 s (6). (B) Time courses for (A) at 348 (solid line), 420 (dotted line), and 495 nm (dashed line). (C) Reaction with 0.5 mM **3** and 5 mM benzaldehyde. Curves are shown at 0.0010 s (1), 4.04 s (2), 12.01 s (3), 24.01 s (4), 48.01 s (5), and 96.01 s (6). (D) Time courses for (C) at 348 (solid line), 420 (dotted line), and 495 nm (dashed line).

all of the proton transfers must occur on one face of the PLP–substrate complex, which is the bottom face of the complexes shown in Scheme 2. This is supported by the stereochemical experiments of Palcic et al., who found that protonation of the enamine occurs with retention of configuration and concluded that the C_β – C_γ bond is oriented syn to the α -CH (18).

Electron-withdrawing groups would favor nucleophilic addition of hydroxide to the γ -carbonyl, while electron-donating substituents would make addition more difficult. Conversely, the stabilizing effect of electron-withdrawing substituents on the *gem*-diolate would make the C_β – C_γ cleavage slower, while electron-donating substituents would be expected to accelerate C_β – C_γ cleavage. The unsubstituted compound or those with weakly electron-donating and electron-withdrawing groups, like *p*-Me and *p*-Cl, balance the formation of the *gem*-diolate and the C_β – C_γ cleavage, whereas the strongly electron-withdrawing group, *p*-CF₃, favors the *gem*-diolate intermediate but reduces the rate of C_β – C_γ

cleavage compared to β -benzoyl-L-alanine. Conversely, the strongly electron-donating *p*-MeO group reduces the rate of formation of the *gem*-diolate but favors the C_β – C_γ cleavage reaction. The stopped-flow kinetic trapping experiments with benzaldehyde show that there is a rough correlation of the k_{cat} values for the β -benzoylalanines with the rates of formation of a quinonoid species absorbing at 494 nm. Benzaldehyde reacts in an aldol-type reaction with the enamine intermediate after benzoate release to form γ -phenylhomoserine (13, 19). However, the very slow 2-substituted substrates (**5**–**7**) react with benzaldehyde with rate constants even slower than k_{cat} .

We found previously that β -benzoyl-L-alanine reacts with kynase to form a new intermediate with a strong absorption peak at about 348 nm ($\epsilon \sim 20000 \text{ M}^{-1} \text{ cm}^{-1}$). This intermediate was not observed in reactions with excess L-kynurenine since the strong absorption of the substrate at 360 nm obscures this region of the spectrum. However, in single turnover stopped-flow experiments,

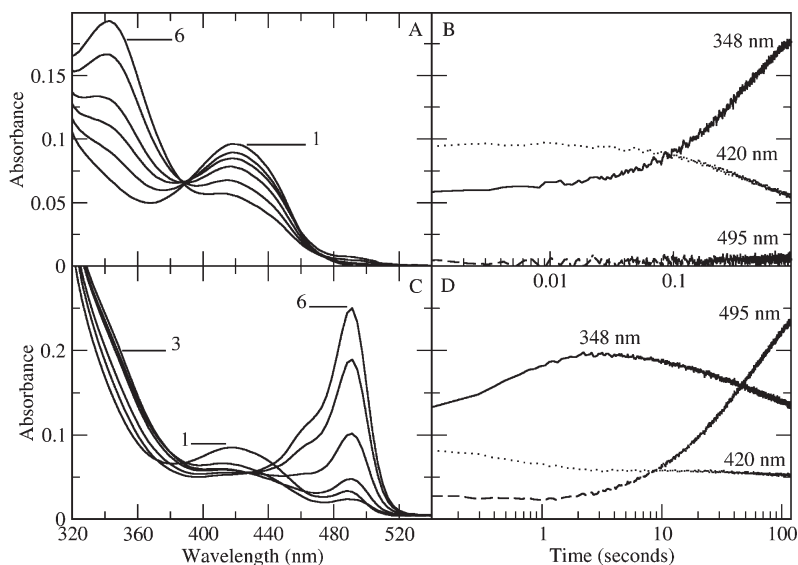


FIGURE 3: Reaction of β -(4-trifluoromethylbenzoyl)-DL-alanine (**4**) with *P. fluorescens* kynase in the stopped-flow spectrophotometer. Reactions contained 1 mg/mL kynase in 40 mM potassium phosphate, pH 8.0, 0.5 mM **4** (A, B, C, and D), and 5 mM benzaldehyde (C and D). (A) Reaction with 0.5 mM **4**. Curves are shown at 0.0002 s (1), 0.0202 s (2), 0.0602 s (3), 0.1202 s (4), 0.2402 s (5), and 0.4802 s (6). (B) Time courses for (A) at 348 nm (solid line), 420 nm (dotted line), and 495 nm (dashed line). (C) Reaction with 0.5 mM **4** and 5 mM benzaldehyde. Curves are shown at 0.00075 s (1), 1.00 s (2), 6.00 s (3), 20.00 s (4), 60.00 s (5), and 120.00 s (6). (D) Time courses for (C) at 348 nm (solid line), 420 nm (dotted line), and 495 nm (dashed line).

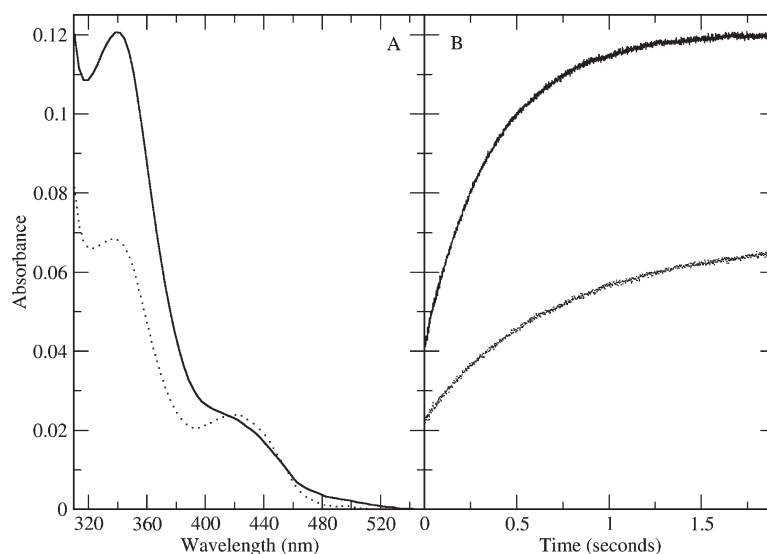


FIGURE 4: (A) Effect of deuteration on the reaction of *P. fluorescens* kynase with 4- CF_3 -benzoylalanine (**4**). Key: solid line, 4- CF_3 -benzoylalanine (0.5 mM); dotted line, β,β - D_2 -4- CF_3 -benzoylalanine. (B) Time courses at 348 nm. Key: solid line, 4- CF_3 -benzoylalanine (0.5 mM); dotted line, β,β - D_2 -4- CF_3 -benzoylalanine.

a transient intermediate with λ_{max} at about 350 nm was observed, which was interpreted at the time as evidence for a ketimine (12) but is likely to be the same species observed in the present work. All of the substituted β -benzoyl-DL-alanines examined in this study also form an intermediate absorbing at about 348 nm, with rate constants similar to that of β -benzoyl-L-alanine, ranging from 2 to 20 s^{-1} (Figures 2A, 3A, and 4A), so the substituent effect on its formation is relatively small. We suggested previously that this intermediate may be the enamine product resulting from C_β - C_γ cleavage (7). However, since the 348 nm intermediate shows a wide range of reactivity with benzaldehyde in the present work (Table 3), that cannot be the case. We now propose that the 348 nm intermediate is a vinylogous amide complex formed by abortive β -deprotonation of the ketimine intermediate (Scheme 2). Vinylogous amides are known to have strong absorptions in the 320–360 nm region, with molar extinction coefficients of

Table 3: Pre-Steady-State Kinetic Rate Constants for Substituted Benzoylalanines

substituent, X	$1/\tau_1$ (s^{-1})	$1/\tau_2$ (s^{-1})
(1) 4-OMe	20 ± 3	0.0174 ± 0.0015
(2) 4-Me	20 ± 1	0.71 ± 0.10
(3) 4-Cl	11.7 ± 0.1	0.24 ± 0.01
(4) 4- CF_3	2.57 ± 0.19 (1.37 ± 0.03) ^a	0.0181 ± 0.0003
(5) 2-Cl	4.52 ± 0.18	0.00285 ± 0.0009
(6) 2-F	14.4 ± 0.5	0.0015 ± 0.0004
(7) 2-OMe	2.74 ± 0.11	— ^c
H	9^b	0.7^b

^a β,β -Dideuterated **4** in parentheses. ^bFrom ref 7. ^cNot determined.

20000–30000 $\text{M}^{-1} \text{cm}^{-1}$ (20). In fact, a compound very similar to the proposed structure of the 348 nm intermediate in Scheme 2,

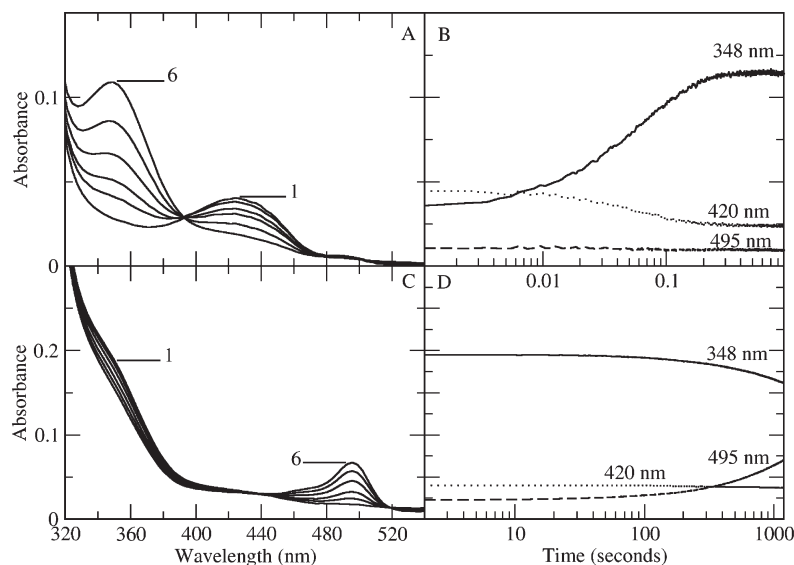
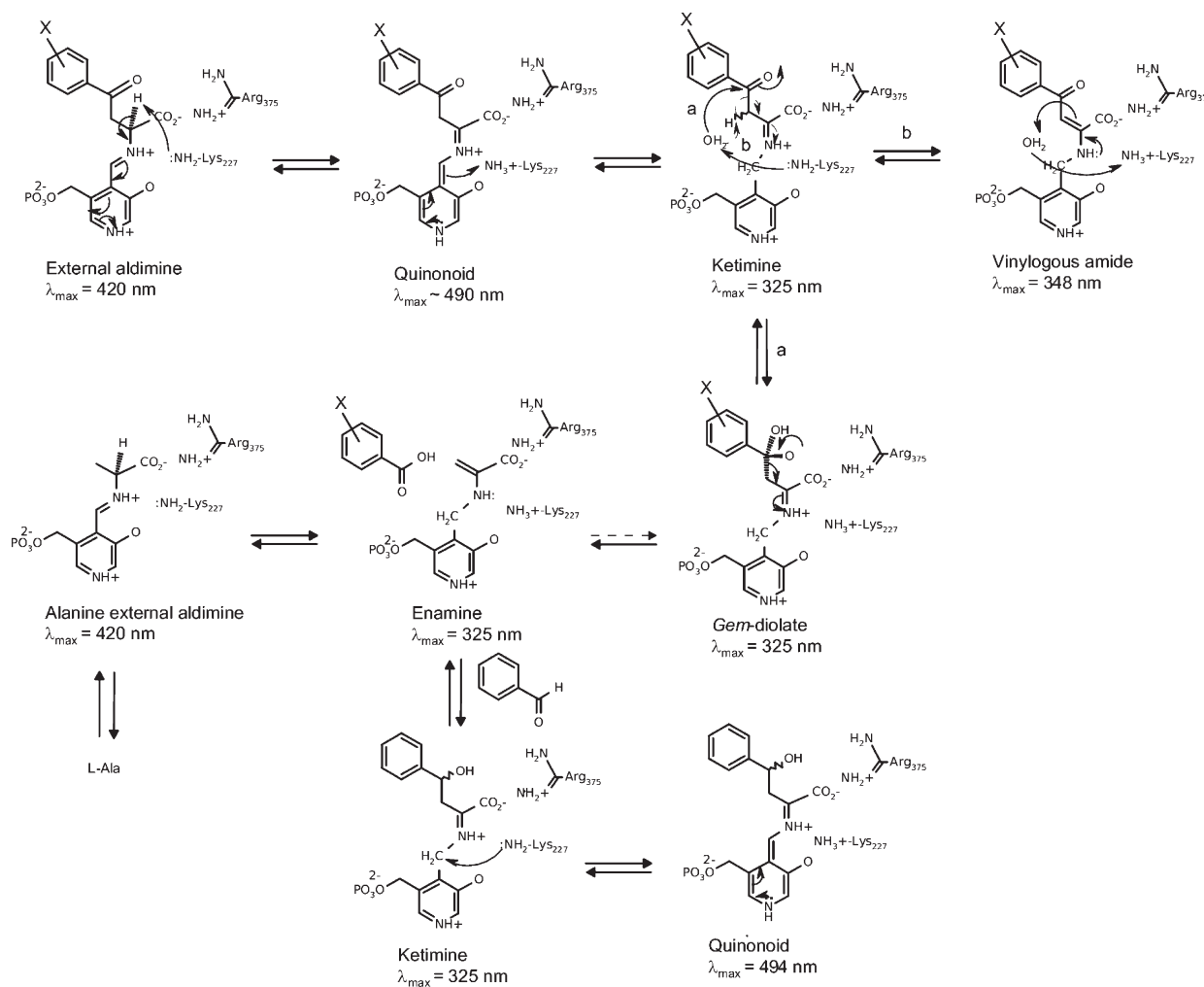


FIGURE 5: Reaction of 2-fluorobenzoyl-DL-alanine (**6**) with *P. fluorescens* kynase in the stopped-flow spectrophotometer. Reactions contained 1 mg/mL kynase in 40 mM potassium phosphate, pH 8.0, 0.5 mM **6** (A, B, C, and D), and 5 mM benzaldehyde (C and D). (A) Reaction with 0.5 mM **6**. Curves are shown at 0.0005 s (1), 0.0205 s (2), 0.0405 s (3), 0.0805 s (4), 0.1605 s (5), and 0.3205 s (6). (B) Time courses for (A) at 348 (solid line), 420 (dotted line), and 495 nm (dashed line). (C) Reaction with 0.5 mM **6** and 5 mM benzaldehyde. Curves are shown at 0.0009 s (1), 12.00 s (2), 30.00 s (3), 60.00 s (4), 90.00 s (5), and 120.00 s (6). (D) Time courses for (C) at 348 (solid line), 420 (dotted line), and 495 nm (dashed line).

Scheme 2: Mechanism of Reaction of β -Benzoylalanines with Kynureninase



3-(N-(2-hydroxyethyl)-N-methylamino)-1-phenyl-1-propenone, exhibits $\lambda_{\max} = 344 \text{ nm}$ and $\epsilon = 23300 \text{ M}^{-1} \text{ cm}^{-1}$ (20). This assignment of the 348 nm intermediate to a vinylogous amide is

supported by the observation of a kinetic isotope effect of 1.88 on its formation from β,β -D₂-4-trifluoromethylbenzoyl-DL-alanine (**4**) (Figure 4). The high absorptivity and the position of the band

are more consistent with the *trans*- rather than the *cis*-vinylogous amide (20). The *trans* geometry is also consistent with the crystal structure of human kynureninase complexed with 3-hydroxyhippuric acid, which shows an extended conformation of the ligand with a *trans*-amide bond (21), and also with docking experiments of 3-hydroxy-L-kynurenine into the active site of human kynureninase (22).

What is the role of this vinylogous amide in the catalytic mechanism of kynase? Previously, we found that the 348 nm intermediate formed from β -benzoyl-L-alanine reacted with benzaldehyde at a rate similar to k_{cat} , so we concluded that it is catalytically competent (7). In earlier pH dependence studies, we proposed that a active site base, possibly the ϵ -amino group of Lys-227, abstracts a proton from a water molecule, and the resulting hydroxide adds to the carbonyl to form the *gem*-diolate (8) (Scheme 2, path a). If the incipient hydroxide abstracts a proton from the β -C of the PMP-ketimine, then instead a vinylogous amide is formed (Scheme 2, path b, dashed arrows). These β -protons should be acidic, since they are located on a carbon between a ketone and an iminium ion. In support of this prediction, the calculated pK_{a} of the CH bond in the β -keto-iminium ion derived from 2,4-pentanedione is 11.90, using the SPARC pK_{a} calculator (23). The absorption intensity of the 348 nm peak suggests that the equilibrium between the *gem*-diolate and the vinylogous amide strongly favors the vinylogous amide. However, the vinylogous amide does not appear to be on the direct catalytic pathway, since it would not allow C_{β} – C_{γ} cleavage, but may be instead a side branch of the mechanism, in rapid equilibrium with the PMP-ketimine. The low reactivity of the 2-substituted benzoylalanines in steady-state kinetics and with benzaldehyde in the stopped-flow experiments may be due to stabilization of the 348 nm abortive complex. In this regard it is interesting that β -(2-methoxybenzoyl)alanine is used as an inhibitor of mammalian kynureninase in vivo (24). Thus, stabilization of the vinylogous amide complex in Scheme 2 is a potential strategy for kynureninase inhibitor design.

Conclusion. There are large electronic effects on the reaction of *P. fluorescens* kynase with substituted β -benzoylalanines. The concave downward Hammett plots indicate a change in rate-determining step from hydration with electron-donating substituents to C_{β} – C_{γ} bond cleavage with electron-withdrawing substituents. These results provide additional evidence for a *gem*-diol intermediate in the catalytic mechanism of kynase. The rapid-scanning stopped-flow data support the conclusions from the steady-state kinetic analysis. A 348 nm intermediate formed in the reaction of these substrates is proposed to be a vinylogous amide not directly on the catalytic pathway.

SUPPORTING INFORMATION AVAILABLE

Details of the synthesis of 2–7 and the pre-steady-state kinetic data for 1, 2, 5, and 7. This material is available free of charge via the Internet at <http://pubs.acs.org>.

REFERENCES

1. Soda, K., and Tanizawa, K. (1979) Kynureninases: Enzymological properties and regulation mechanism. *Adv. Enzymol. Relat. Areas Mol. Biol.* 49, 1–40.
2. Hayaishi, O., and Stanier, R. Y. (1951) The bacterial oxidation of tryptophan III: Enzymatic activities of cell-free extracts from bacteria employing the aromatic pathway. *J. Bacteriol.* 62, 691–709.
3. Koushik, S. V., Sundaraju, B., McGraw, R. A., and Phillips, R. S. (1997) Cloning, sequence, and expression of kynureninase from *Pseudomonas fluorescens*. *Arch. Biochem. Biophys.* 344, 301–308.
4. Achim, C. L., Heyes, M. P., and Wiley, C. A. (1993) Quantitation of human immunodeficiency virus, immune activation factors, and quinolinic acid in AIDS brains. *J. Clin. Invest.* 91, 2769–2775.
5. Sei, S., Saito, K., Stewart, S. K., Crowley, J. S., Brouwers, P., Kleiner, D. E., Katz, D. A., Pizzo, P. A., and Heyes, M. P. (1995) Increased human immunodeficiency virus (HIV) type 1 DNA content and quinolinic acid concentration in brain tissues from patients with HIV encephalopathy. *J. Infect. Dis.* 172, 638–647.
6. Stone, T. W. (2000) Inhibitors of the kynurenine pathway. *Eur. J. Med. Chem.* 35, 179–186.
7. Gawandi, V. B., Liskey, D., Lima, S., and Phillips, R. S. (2004) Reaction of *Pseudomonas fluorescens* kynureninase with beta-benzoyl-L-alanine: Detection of a new reaction intermediate and a change in rate-determining step. *Biochemistry* 43, 3230–3237.
8. Koushik, S. V., Moore, J. A., III, Sundaraju, B., and Phillips, R. S. (1998) The catalytic mechanism of kynureninase from *Pseudomonas fluorescens*: Insights from the effects of pH and isotopic substitution on steady-state and pre-steady-state kinetics. *Biochemistry* 37, 1376–1382.
9. Cleland, W. W. (1979) Statistical analysis of enzyme kinetic data. *Methods Enzymol.* 63, 103–138.
10. Matheson, I. B. C., and DeSa, R. J. (1990) Robust multicomponent analysis applied to the separation of components in a mixture of absorbing species. *Comput. Chem.* 14, 49–57.
11. Kosower, E. M., Cole, W. J., Wu, G.-S., Cardy, D. E., and Meisters, G. (1963) Halogenation with copper(II). I. Saturated ketones and phenol. *J. Org. Chem.* 28, 630–633.
12. Phillips, R. S., Sundaraju, B., and Koushik, S. V. (1998) The catalytic mechanism of kynureninase from *Pseudomonas fluorescens*: Evidence for transient quinonoid and ketimine intermediates from rapid-scanning stopped-flow spectrophotometry. *Biochemistry* 37, 8783–8789.
13. Phillips, R. S., and Dua, R. K. (1991) Stereochemistry and mechanism of aldol reactions catalyzed by kynureninase. *J. Am. Chem. Soc.* 113, 7385–7388.
14. Dua, R. K., Taylor, E. W., and Phillips, R. S. (1993) S-Aryl-L-cysteine S,S-dioxides: Design and evaluation of a new class of mechanism based inhibitors of kynureninase. *J. Am. Chem. Soc.* 115, 1264–1270.
15. Heiss, C., Anderson, J., and Phillips, R. S. (2003) Differential effects of bromination on substrates and inhibitors of kynureninase from *Pseudomonas fluorescens*. *Org. Biomol. Chem.* 1, 288–295.
16. Tanizawa, K., and Soda, K. (1979) The mechanism of kynurenine hydrolysis catalyzed by kynureninase. *J. Biochem. (Tokyo)* 86, 1199–1209.
17. Dunathan, H. C. (1971) Stereochemical aspects of pyridoxal phosphate catalysis. *Adv. Enzymol. Relat. Areas Mol. Biol.* 35, 79–134.
18. Palcic, M. M., Antoun, M., Tanizawa, K., Soda, K., and Floss, H. G. (1985) Stereochemistry of the kynureninase reaction. *J. Biol. Chem.* 260, 5248–5251.
19. Bild, G. S., and Morris, J. C. (1984) Detection of beta-carbanion formation during kynurenine hydrolysis catalyzed by *Pseudomonas marginalis* kynureninase. *Arch. Biochem. Biophys.* 235, 41–47.
20. King, L. C., and Ostrum, G. K. (1964) Vinylogous imides. 11. Ultraviolet spectra and the application of Woodward's rules. *J. Org. Chem.* 29, 3459–3461.
21. Lima, S., Kumar, S., Gawandi, V., Momany, C., and Phillips, R. S. (2009) Crystal structure of the *Homo sapiens* kynureninase-3-hydroxyhippuric acid inhibitor complex: Insights into the molecular basis of kynureninase substrate specificity. *J. Med. Chem.* 52, 389–396.
22. Lima, S., Khristoforov, R., Momany, C., and Phillips, R. S. (2007) Crystal structure of *Homo sapiens* kynureninase. *Biochemistry* 46, 2735–2744.
23. Hilal, S., Karickhoff, S. W., and Carreira, L. A. (1995) A rigorous test for SPARC's chemical reactivity models: Estimation of more than 4300 ionization pK_{a} 's. *Quant. Struct.-Act. Relat.* 14, 348.
24. Chiarugi, A., Carpenedo, R., and Moroni, F. (1996) Kynurenine disposition in blood and brain of mice: Effects of selective inhibitors of kynurenine hydroxylase and of kynureninase. *J. Neurochem.* 67, 692–698.